

EDA R-matrix evaluations for light-elements

Nuclear Data Week/CSEWG
Evaluations session

Mark Paris & Gerry Hale

2020-12-01



Managed by Triad National Security, LLC for the U.S. Department of Energy's NNSA

LA-UR-20-29796

Motivation & Outline

- **Updating evaluation sublibraries**

- **Neutron:** n-001_H_001.endf, n-003_Li_006.endf, n-004_Be_009.endf
- **Proton:** p-001_H_001.endf, p-002_He_004.endf
- **Deuteron:** d-002_He_003.endf
- **Triton:** t-002_He_004.endf

- **Motivation:** improve fidelity of charged-particle and n-induced evaluations

- **Validation:** IAEA; NJOY; pencil-beam; quasi-int. (Danon); Faust (Herman)

- **EDA** evaluation pipeline

- Overview/reminder

- **High-fidelity, unitary R-matrix** approach

- Simultaneous evaluation of **all** data

- Evaluation reproduction

- Challenges in push-button/script-driven reproducibility for our approach

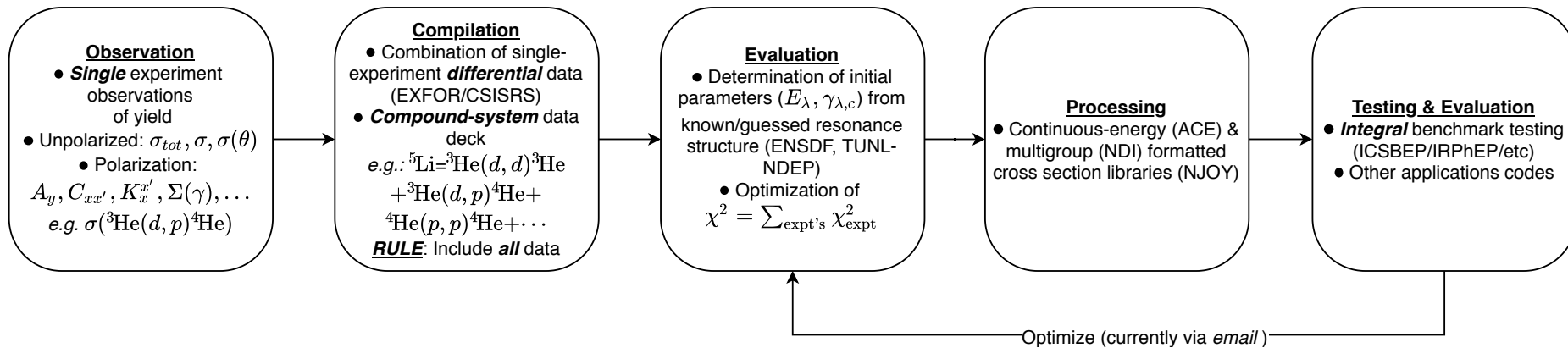
- **NB:** our evaluation approach is currently heavily hand-spun

- Automation *limited* but *under development*

Overview

Light-element evaluation

Nuclear Data Pipeline EDA cross section evaluation



- Data-cull: observables from single experiments are compiled
- Evaluation: one set of variational parameters for all data
 - Unitary parametrization: highly constraining between different processes
 - Elastic & reaction cross sections are coupled in complex ways
 - Not simply drawing smooth curves
- Processing/Verification/Validation

Uncertainties from chi-squared minimization

$$\chi_{\text{EDA}}^2 = \sum_i \left[\frac{nX_i(\mathbf{p}) - R_i}{\Delta R_i} \right]^2 + \left[\frac{nS - 1}{\Delta S / S} \right]^2$$

$$\begin{cases} R_i, \Delta R_i = \text{relative measurement, uncertainty} \\ S, \Delta S = \text{experimental scale, uncertainty} \\ X_i(\mathbf{p}) = \text{observable calc. from res. pars. } \mathbf{p} \\ n = \text{normalization parameter} \end{cases}$$

Near a minimum of the chi-squared function at $\mathbf{p} = \mathbf{p}_0$:

$$\begin{aligned} \chi^2(\mathbf{p}) &= \chi_0^2 + (\mathbf{p} - \mathbf{p}_0)^T \mathbf{g}_0 + \frac{1}{2} (\mathbf{p} - \mathbf{p}_0)^T \mathbf{G}_0 (\mathbf{p} - \mathbf{p}_0) \\ &= \chi_0^2 + \Delta\chi^2. \end{aligned}$$

$$\begin{cases} \chi_0^2 = \chi^2(\mathbf{p}_0) \\ \mathbf{g}_0 = \nabla_{\mathbf{p}} \chi^2(\mathbf{p}) \Big|_{\mathbf{p}=\mathbf{p}_0} \approx 0 \\ \mathbf{G}_0 = \nabla_{\mathbf{p}} \mathbf{g}(\mathbf{p}) \Big|_{\mathbf{p}=\mathbf{p}_0} \end{cases}$$

Conventions:

1) previous: $\Delta\chi^2 = 1 \implies$ Very small uncertainties $\delta p_i = (C_{ii}^0)^{1/2} \sim \mathcal{O}(N_p^{-1/2})$

2) improved: $\Delta\chi^2 = \frac{1}{2} \Delta\mathbf{p}^T \mathbf{G}_0 \Delta\mathbf{p} \leq \Delta\chi_{\text{max}}^2$,

$$P(\Delta\chi^2 | k) = \left[2^{\frac{k}{2}} \Gamma\left(\frac{k}{2}\right) \right]^{-1} \int_0^{\Delta\chi_{\text{max}}^2} t^{\frac{k}{2}-1} e^{-t/2} dt = \text{CL (e.g. } \sim 0.68 \text{ for } 1\text{-}\sigma, 0.95 \text{ for } 2\text{-}\sigma, \text{ etc.)}$$

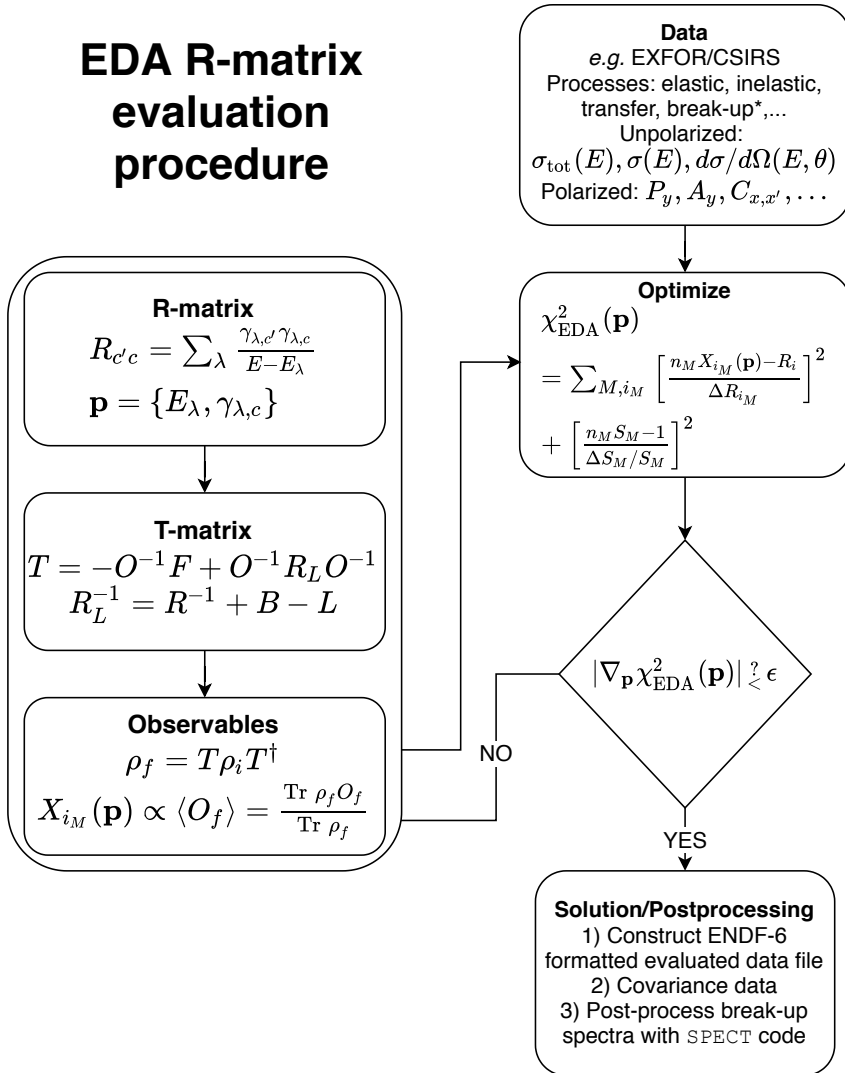
$$\Delta\chi_{\text{max}}^2 \approx k = \langle \Delta\chi^2 \rangle.$$

$$\delta p_i \sim (N_p C_{ii}^0)^{1/2}$$

R-matrix evaluation

⁵Li system

EDA R-matrix evaluation procedure



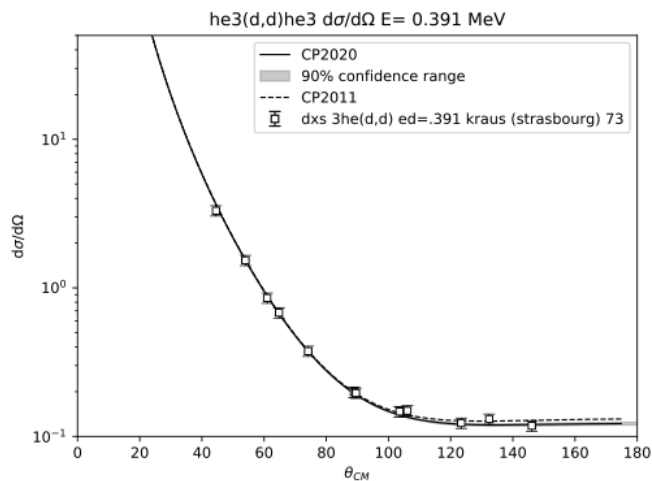
Channel	a_c (fm)	l_{max}
$d + {}^3\text{He}(\frac{1}{2}^+)$	4.8	4
$p + {}^4\text{He}(0^+)$	2.9	4
$p + {}^4\text{He}^*(0^+; 20.2 \text{ MeV})$	3.4	2
$d_0 + {}^3\text{He}(\frac{1}{2}^+)$	5.1	0

Reaction	Energy Range (MeV)	# Data Points	Observables
${}^3\text{He}(d, d){}^3\text{He}$	$E_d = 0.32 - 10.0$	2,229	$\sigma(\theta), A_i, A_{ii}, C_{i,j}, C_{ij,k}, K_{i,j'k'}, K_{ij,k'l'}$
${}^3\text{He}(d, p){}^4\text{He}$	$E_d = 0.13 - 10.0$	3,839	$\sigma(E), \sigma(\theta), A_i, A_{ii}, C_{i,j}, K_{ij,k'}$
${}^3\text{He}(d, p){}^4\text{He}^*$	$E_d = 3.70 - 6.70$	28	$\sigma(\theta)$
${}^4\text{He}(p, p){}^4\text{He}$	$E_p = 0.92 - 34.3$	867	$\sigma(E), \sigma(\theta), A_y, P_y$
Total:		6963	

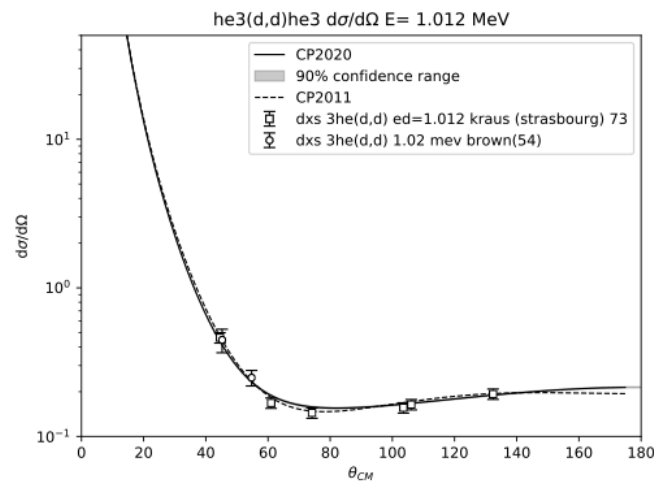
Table 1: Channel configuration (top) and data summary (bottom) for the ⁵Li system analysis. The column labeled “Observables” indicates the following data types: $\sigma(E)$, integrated cross section; $\sigma(\theta)$, unpolarized angular distributions (energy-dependence suppressed); A initial-state analyzing power; P final-state polarization; C spin correlation coefficients; K polarization transfer coefficients. (We have suppressed the indices i, j, \dots which take on values x, y, z for spins/polarization directions in configuration space.) All polarization and spin distributions are angular distributions, which depend on the angle of the outgoing particle. Chi-squared per degree of freedom for the analysis is $\chi^2/\text{dof} \simeq 2.7$ over 7,178 data points, 215 of which were discarded by eliminating individual data points which contribute to $\chi^2 > 40$.

^5Li system evaluation

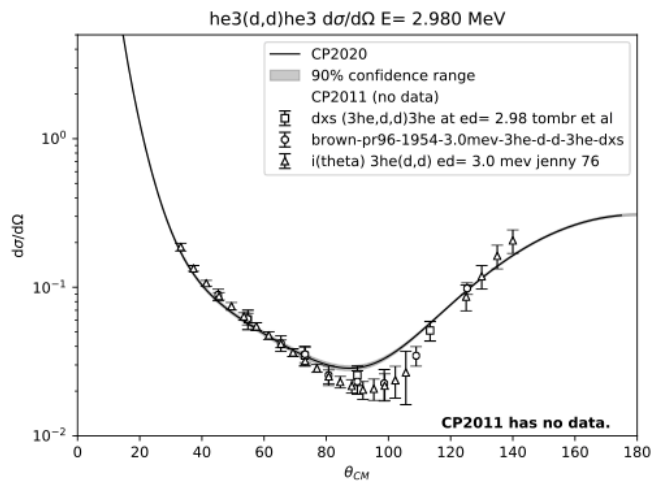
$^3\text{He}(d,d)^3\text{He}$



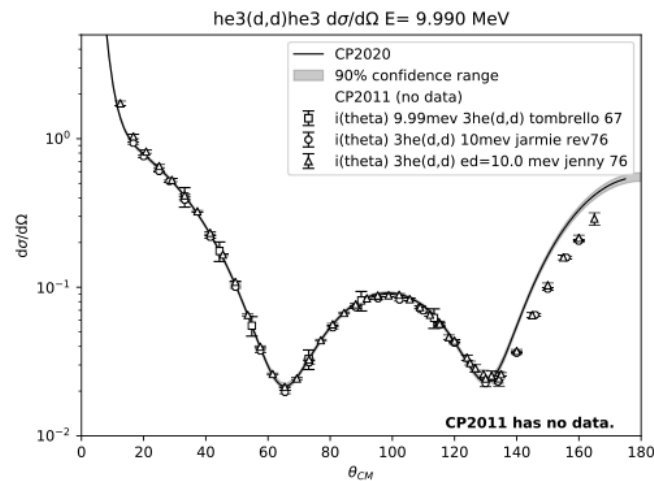
(a)



(b)



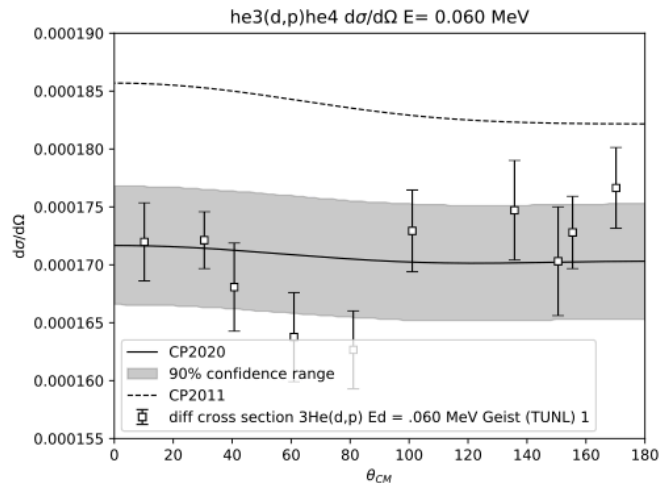
(c)



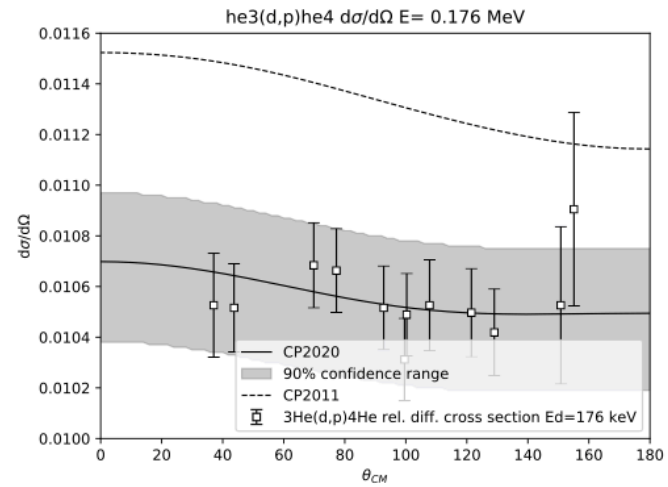
(d)

^5Li system evaluation

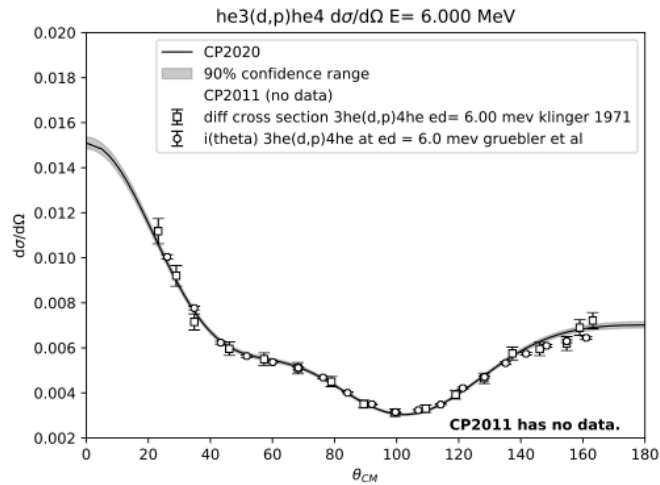
$^3\text{He}(d,p)^4\text{He}$



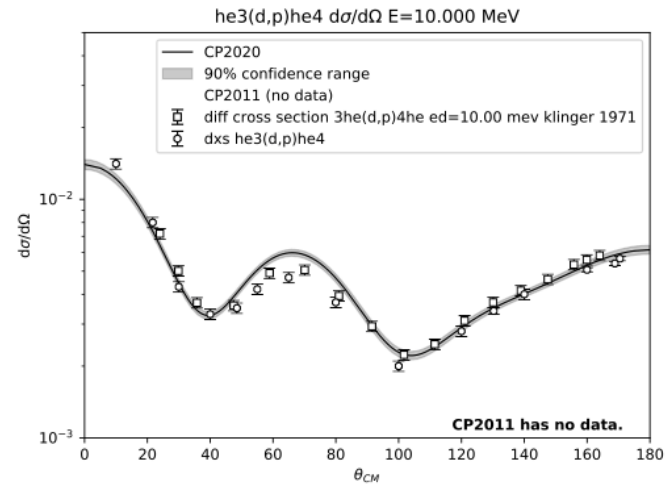
(a)



(b)



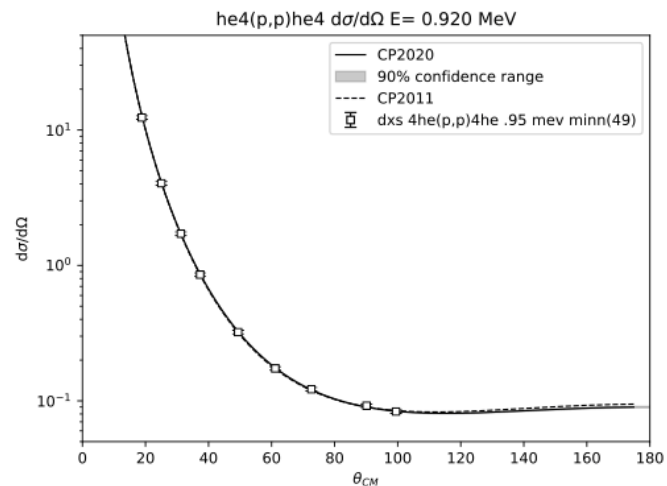
(c)



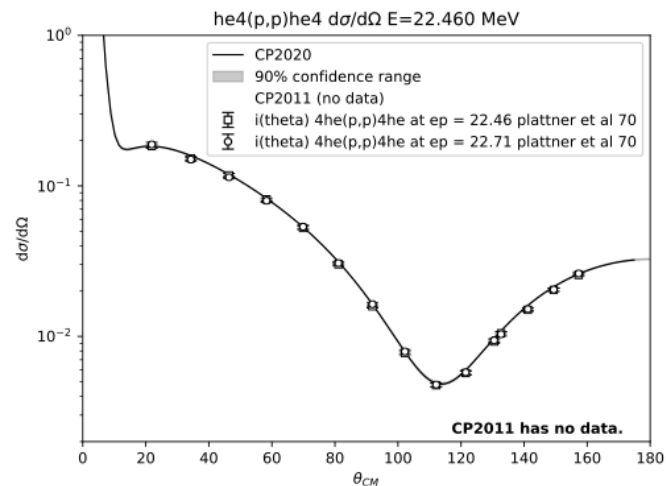
(d)

^5Li system evaluation

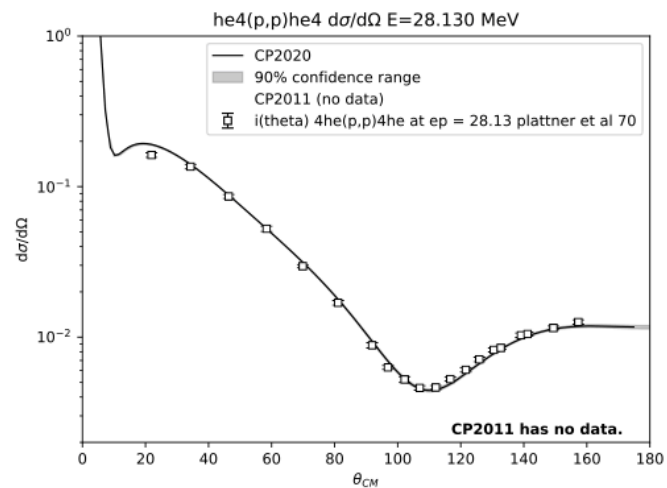
$^4\text{He}(p,p)^4\text{He}$



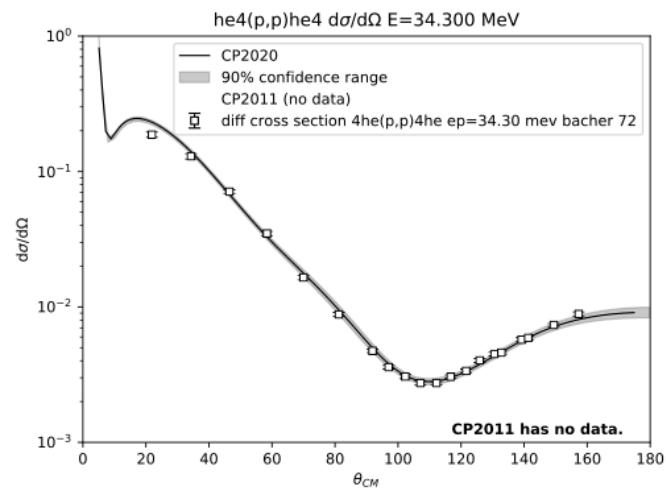
(a)



(b)



(c)



(d)

NN evaluation: configuration & data

- Neutron energies $E_n \leq 50$ MeV
- Charge-independent analysis

$$R(E) = \sum_{\lambda, T} \frac{\gamma_{\lambda}^{(T)} \tilde{\gamma}_{\lambda}^{(T)}}{E_{\lambda}^{(T)} - E}$$

- T=1 (pp, np-isovector)
- T=0 (np-isoscalar)
- Coulomb energy-level shift

$$E_{\lambda}^{(T=1)} = E^{(T=0)} + \Delta_Z$$

- Fit to $a_{nn} = -18.5$ fm
- Predict nn scattering
- High-fidelity description

$$\chi^2/\text{dof} = 0.9$$

- Planned evaluation
 - $E_n \lesssim 250$ MeV

TABLE II. Channel configuration (top) and data summary (bottom) for the charge-independent $N - N$ analysis up to 50 MeV. Since the number of free parameters is 43 resonance parameters + 83 normalizations, the chi-squared per degree of freedom for the analysis is 0.90.

Channel	a_c (fm)	l_{\max}
$p + p$	3.26	3
$n + p$	3.26	3
$\gamma + d$	84.6	1
$n + n$	3.26	3

Reaction	# Pts.	χ^2	Observable Types
$p(p, p)p$	675	951	$\sigma(\theta), A_y(p), C_{x,x'}, C_{y,y'}, K_x^{x'}, K_y^{y'}, K_z^{x'}$
$p(n, n)p$	4815	3764	$\sigma_T, \sigma(\theta), A_y(n), C_{y,y'}, K_y^{y'}$
$p(n, \gamma)d$	86	179	$\sigma_{\text{int}}, \sigma(\theta), A_y(n)$
$d(\gamma, n)p$	88	77	$\sigma_{\text{int}}, \sigma(\theta), \Sigma(\gamma), P_y(n)$
$n(n, n)n$	1	0	a_0
Norms.	80	86	
Total:	5745	5057	20

Integrated cross sections

Comparison with ENDF/B-VIII.0

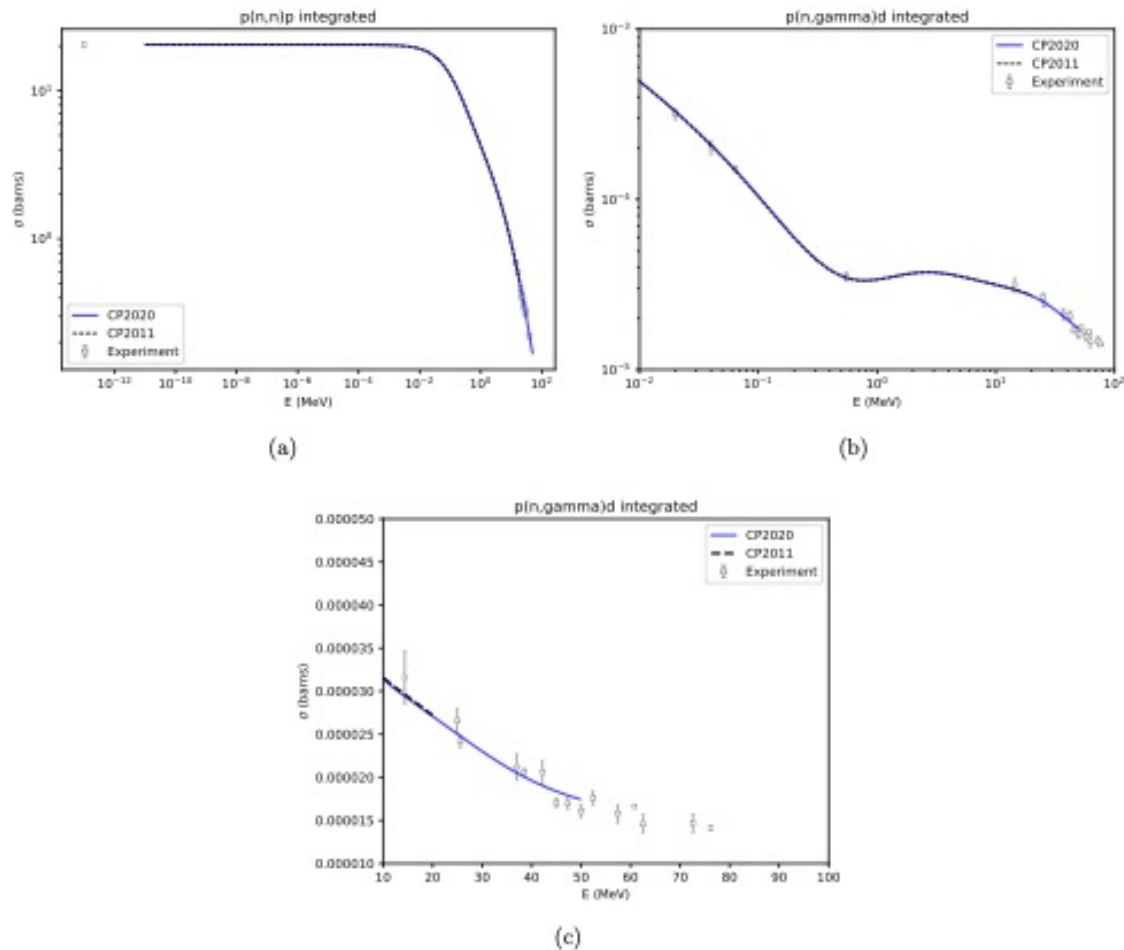
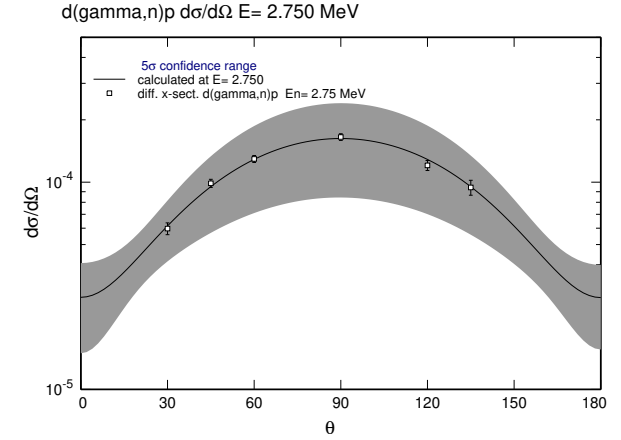
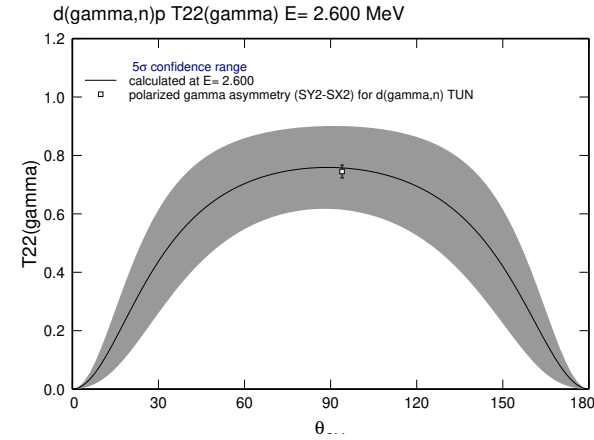
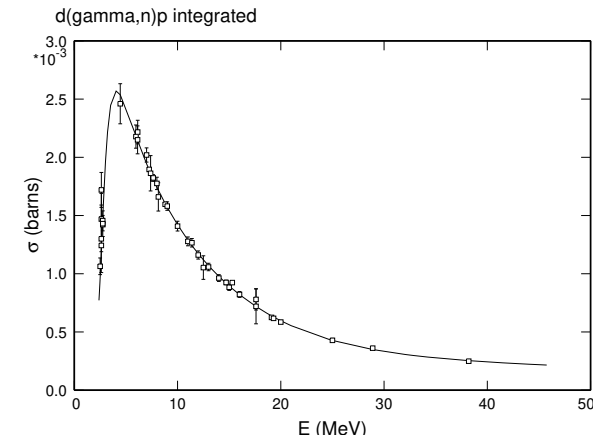
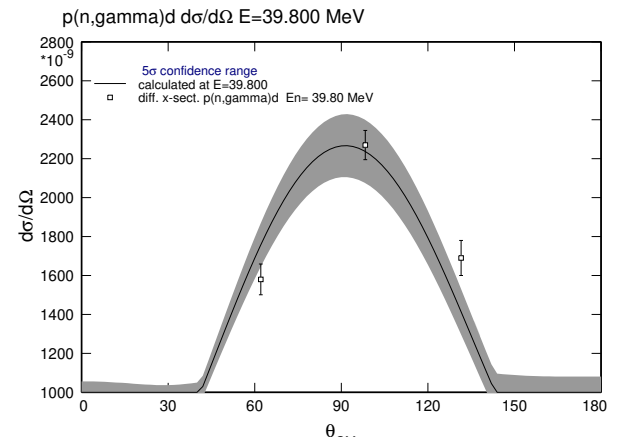
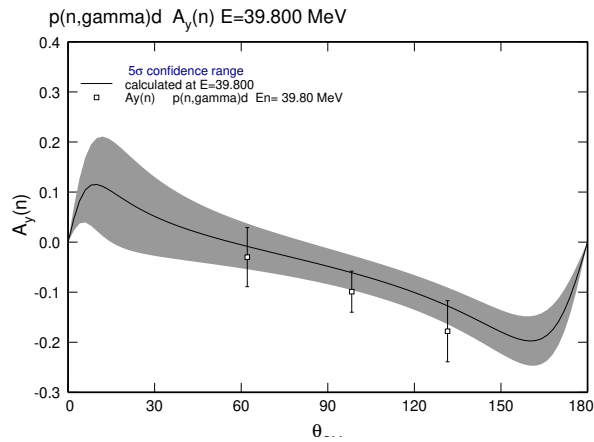
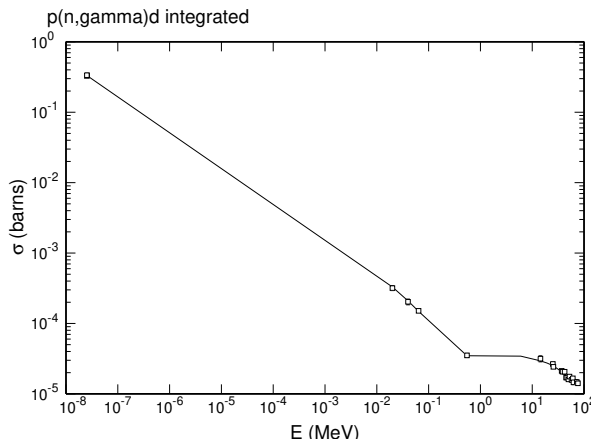


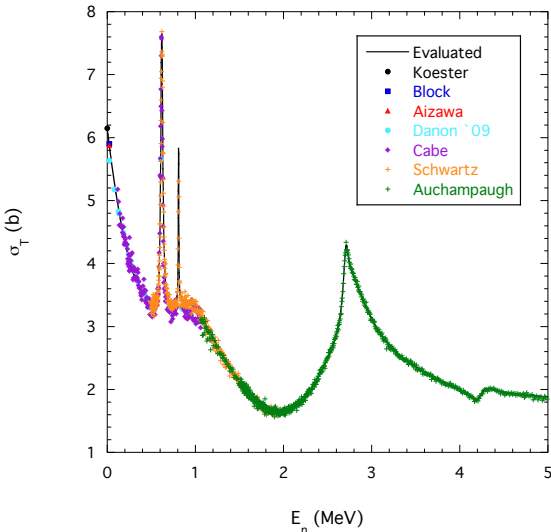
Figure 6: The CP2020 integrated cross sections (solid, blue curves) compared with those of CP2011 (dashed curves) and the experimentally observed data for: (a) ${}^1\text{H}(n, n){}^1\text{H}$ reaction; (b) ${}^1\text{H}(n, \gamma){}^2\text{H}$ reaction; (c) ${}^1\text{H}(n, \gamma){}^2\text{H}$ reaction (focus on high-energy region). The capture process ${}^1\text{H}(n, \gamma){}^2\text{H}$ has not yet been updated in an ENDF file for CP2020.

n+p Capture and γ +d Photodisintegration Data

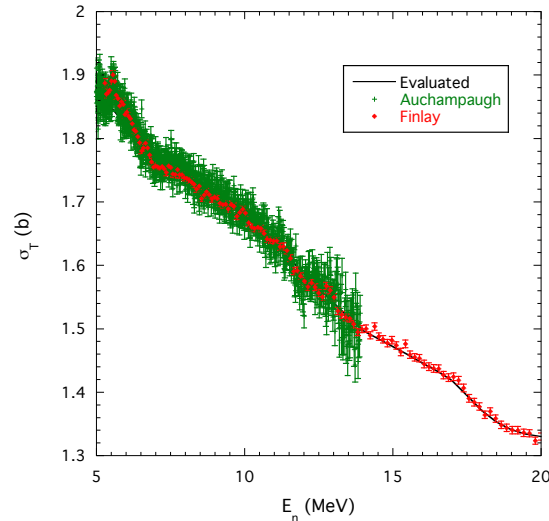


n+⁹Be Integrated Cross Sections

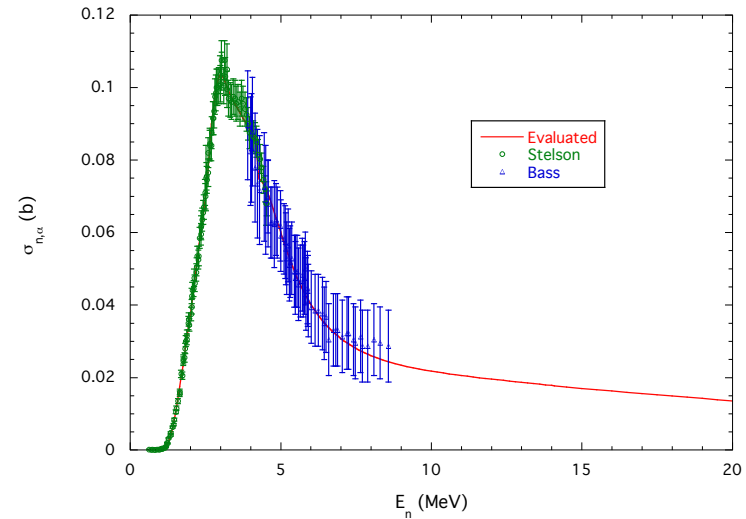
n+⁹Be Total Cross Section



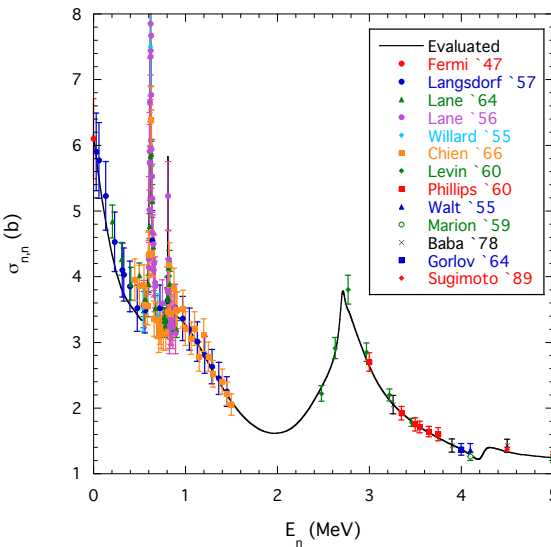
n+⁹Be Total Cross Section



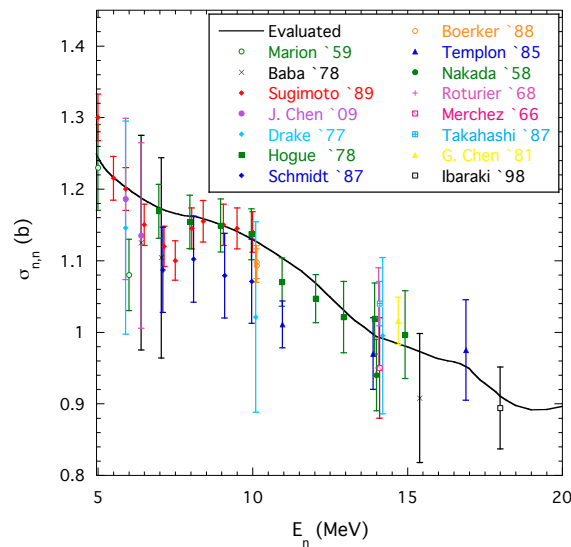
⁹Be(n,α)⁶He Cross Section



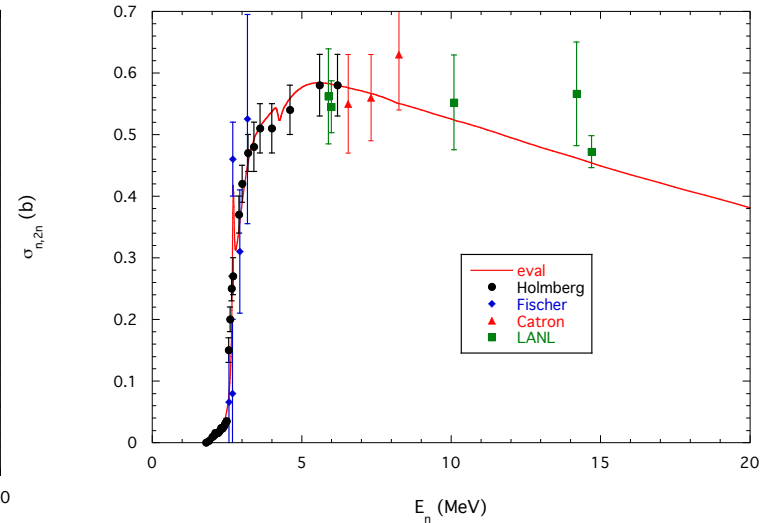
⁹Be(n,n)⁹Be Cross Section



⁹Be(n,n)⁹Be Cross Section

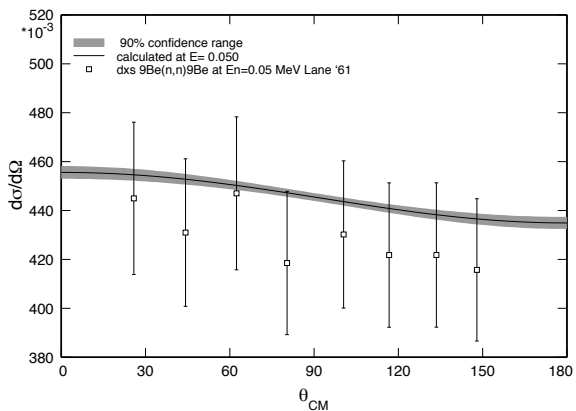


⁹Be(n,2n)αα Cross Section

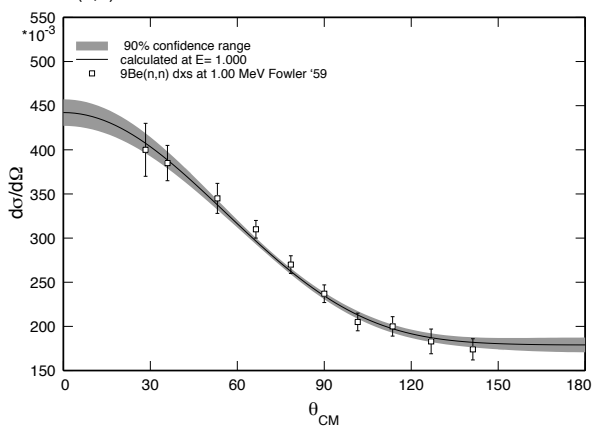


${}^9\text{Be}(n,n){}^9\text{Be}$ Differential Cross Sections

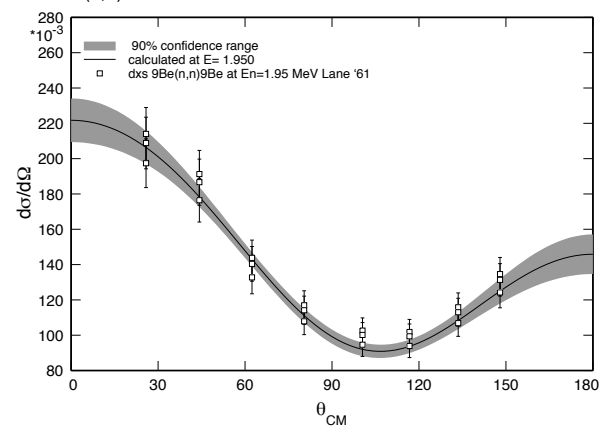
${}^9\text{Be}(n,n){}^9\text{Be}$ $d\sigma/d\Omega$ $E= 50.000$ keV



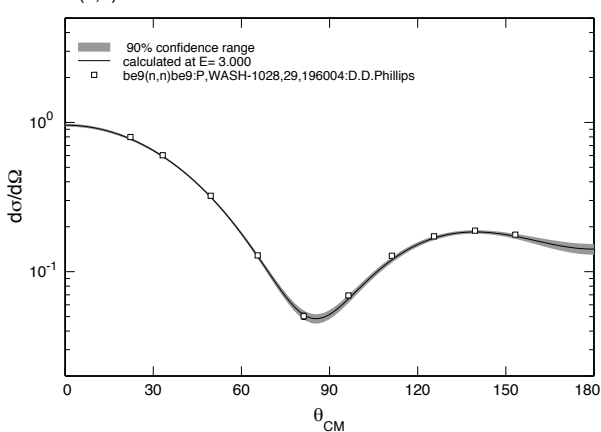
${}^9\text{Be}(n,n){}^9\text{Be}$ $d\sigma/d\Omega$ $E= 1.000$ MeV



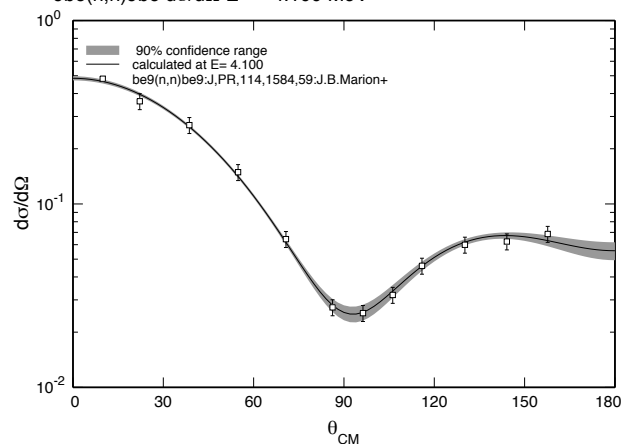
${}^9\text{Be}(n,n){}^9\text{Be}$ $d\sigma/d\Omega$ $E= 1.950$ MeV



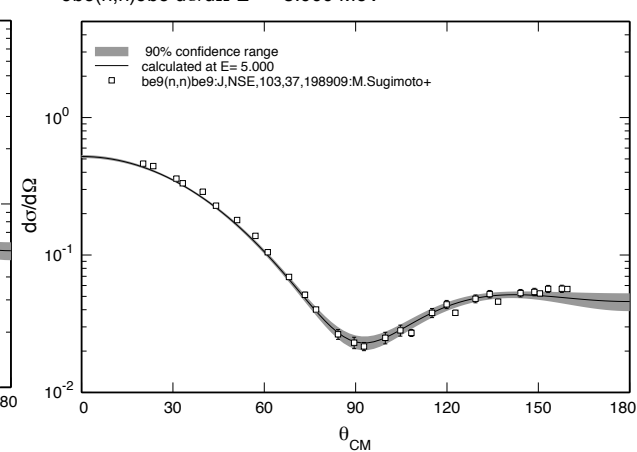
${}^9\text{Be}(n,n){}^9\text{Be}$ $d\sigma/d\Omega$ $E= 3.000$ MeV



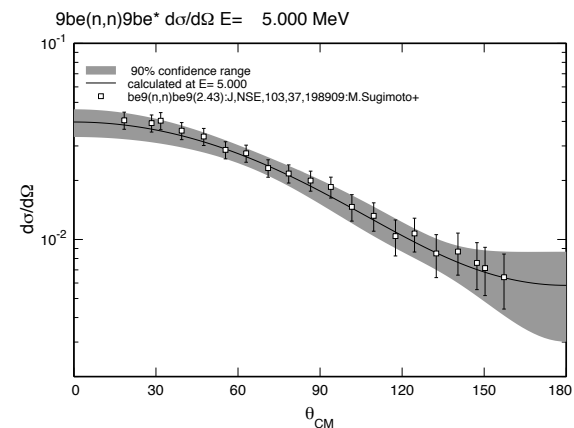
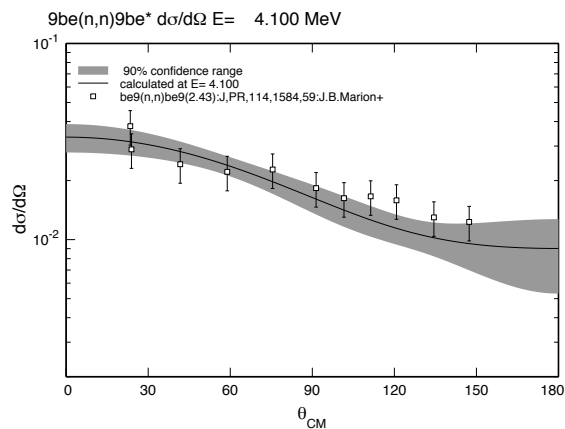
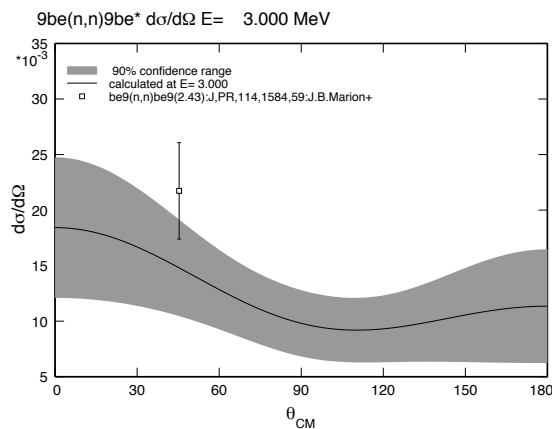
${}^9\text{Be}(n,n){}^9\text{Be}$ $d\sigma/d\Omega$ $E= 4.100$ MeV



${}^9\text{Be}(n,n){}^9\text{Be}$ $d\sigma/d\Omega$ $E= 5.000$ MeV



${}^9\text{Be}(n,n_2){}^9\text{Be}^{**}$ Differential Cross Sections



SUMMARY:

- ${}^{10}\text{Be}$ analysis has produced a consistent set of cross sections and angular distributions that are in agreement with most of the experimental data at energies up to 5 MeV. Extensions above that energy were based on the experimental data alone.
- Level assignments for the overlapping resonances near $E_n = 2.7$ MeV have the opposite parity ($4^-, 3^+ \rightarrow 4^+, 3^-$).
- Excited states of ${}^9\text{Be}$ make important contributions to the $(n,2n)$ cross section ($MT = 16 \rightarrow 24$ in the new evaluation).
- We are making comparisons of the new evaluation to integral benchmarks (M. Herman, LANL) and thick-target angular neutron yields (Y. Danon, RPI).



Thank you.